A Subnanosecond Pulsed Electric Field System for Studying Cells Electropermeabilization

Njomza Ibrahimi, *Student Member, IEEE,* Leslie Vallet, Franck Andre, Laurent Ariztia, Marc Rivaletto, Antoine Silvestre de Ferron, Bucur M. Novac, *Senior Member, IEEE,* Lluis M. Mir, and Laurent Pécastaing, *Senior Member, IEEE*

***Abstract*—This paper presents an experimental arrangement which, using 3-D numerical modeling, aims to study biomedical effects using subnanosecond pulsed electric fields. As part of a major effort into developing contactless technology, the final aim of this study is to determine the strength and pulse repetition frequency of the applied pulsed electric fields required to produce electropermeabilization. The arrangement uses a pulsed power generator producing voltage impulses with an amplitude of up to 20 kV on a 50 Ω matched load, with a rise time of 100 ps and a duration of 600 ps. During the preliminary study reported here, samples containing *E. Coli* were exposed to pulsed electric fields in a 4 mm standard electroporation cuvette, allowing the application of a peak electric field strength of up to 60 kV/cm. The studies were facilitated by detailed 3-D electromagnetic modeling of the electric field distribution generated by voltage impulses inside the system. Due to the nature of tests, the numerical analysis played an essential role in the interpretation of results. Preliminary biological results reported in this study are very encouraging, showing that trains of 5000 to 50000 pulses applied at a pulsed repetition frequency of 200 Hz can efficiently induce *E. Coli* electropermeabilization.**

***Index Terms*—pulsed electric fields, biological cells, subnanosecond pulses, electropermeabilization, pulsed power**

I. Introduction

THE use of narrow-band electromagnetic fields for application to medicine and biology has received significant attention by the scientific community over the last few decades [1]. Electroporation (electric pore formation) is a phenomenon which increases the permeability of the cell membrane when exposed to pulsed electric fields (PEFs) of high intensity and short duration. The pore formation generates openings in the cell membrane, allowing for the transfer of therapeutic molecules across the cell membrane [2], [3]. Thus, the electroporation phenomenon contributes to the efficiency of electrochemotherapy, when used with drugs [4] and electrogenetherapy, when used with DNA plasmids [5].

PEFs can cause reversible electroporation i.e., a temporary permeabilization of the cell membrane [6], but they can also produce irreversible electroporation i.e., cell death, for eradicating cancerous or other unwanted cells [7].

There are basically two types of PEF techniques applied in vivo: *invasive*, where metallic pairs of penetrating electrodes are used to apply the electric field and *noninvasive*, where the electric field is generated through electrodes brought in contact with the skin, without penetration of the body. In addition, the *contactless* term refers here to the approach dealing with the generation of electric fields remotely from the metallic structure of a *PEF source (antenna)*.

The *electrode-based contact* technology is already successfully applied in the treatment of various cancers including, but not limited to kidney, liver, lung and bone cancers [8]. Pulses having hundred of ns duration applied for cancer treatment are still under clinical trials and as such are not part of regular treatments. PEFs of about 100 μs are widely used, depending on the type and the evolution of cancer while ms pulses are not used for cancer treatment. The outcome effect depends not only on the magnitude and duration of the PEFs delivered, but also on the pulse repetition frequency (PRF) and on the characteristics of the tissue, in particular its conductivity. Closer to the subject of the present work, irreversible electroporation using submicrosecond very high intensity PEFs in the tissues is widely considered in many hospitals. An advantage of this technique is that the thermal effects are considerably lower, when compared to other ablation techniques [9]. Cancer treatment techniques, which include but are not limited to chemotherapy and surgery, are unfortunately accompanied by adverse side effects imposed on the patient [10], [11]. The future of the PEF-based cancer treatment techniques is therefore closely related to the identification of new ways to avoid the challenges imposed by the existing *invasive* surgical procedure. The pathway towards a *contactless* technology, a non-surgical procedure, which aims at overcoming some of the issues mentioned above, was studied in very few research laboratories worldwide. The reason for the very limited number of publications published in this domain is perhaps due to the fact that, depending on their output voltage, the highly specialized HV subnanosecond pulsed

Manuscript received August 27, 2020. This work was supported by Agence Nationale de la Recherche (ANR), under Contract No. ANR-18-ASTR-0019.

N. Ibrahimi, L. Ariztia, M. Rivaletto, A. S. de Ferron and L. Pécastaing are with the Université de Pau et des Pays de l'Adour/ E2S UPPA, Laboratoire des Sciences de l'Ingénieur Appliquées à la Mécanique et au Génie Électrique – Fédération IPRA, EA4581, 64000, Pau, France (e-mail: laurent.pecastaing@univ-pau.fr).

L. Vallet, F. Andre and L. M. Mir are with the Université Paris-Saclay, Institut Gustave Roussy, CNRS, Metabolic and Systemic Aspects of Oncogenesis (METSY) 94805 Villejuif, France (e-mail: Luis.MIR@cnrs.fr).

B. M. Novac is with the Wolfson School of Mechanical, Electrical and Manufacturing Engineering, Loughborough University, Loughborough LE11 3TU, U.K. and with the Université de Pau et des Pays de l'Adour/ E2S UPPA, Laboratoire des Sciences de l'Ingénieur Appliquées à la Mécanique et au Génie Électrique – Fédération IPRA, EA4581, 64000, Pau, France (e-mail: b.m.novac@lboro.ac.uk).

power generators required are either extremely expensive or only available at military related research centers. Even more difficult, the focusing of electromagnetic radiation with very high precision in a volume around 1 cm^3, or preferably even lower, is possible only using highly sophisticated impulse antenna techniques.

Two possible solutions were suggested theoretically by Carl Baum, as part of a major research effort undertook by the Frank Reidy Research Center for Bioelectrics at Old Dominion University (USA): an impulse radiating antenna (IRA) operated in air [12], [13], in combination with a complex many layer dielectric lens [14] and another prolate-spheroidal reflector, operated underwater [15]. More recently, at the same research center, a dielectric rod antenna was also suggested as a candidate for generating subnanosecond PEFs for the stimulation of neurological tissue [16]. All the three techniques have been theoretically investigated using CST software [15], [16], [17], with detailed numerical studies being reported. In contrast, very limited experimental work has been published, and only using rather low voltage subnanosecond pulsed power generators, with the resulting PEFs having extremely low peak values when compared with the values required for electroporation [18], [19], [20], the latter work representing an effort made at University of Limoges (France). For stimulating deep inside a tissue, say at 8 cm [17] using intense PEFs of some tens of kV/cm, published work suggest a subnanosecond pulsed power generator with a peak output voltage in excess of 250 kV is required [17]. Such a generator is technically extremely challenging.

Another aspect is that when using such innovative *contactless* delivery systems, the characteristics of the subnanosecond PEFs are different when compared with those of the existing PEF processing. A logical step is therefore to understand their action on cells by firstly using standard electrode-based PEFs driven by subnanosecond pulsed power generators. Results published by the Old Dominion team and also by a research group at Chongqing University (P.R. China), demonstrated that subnanosecond PEFs can indeed produce: permeabilization [21] followed by the transfer of molecules inside the cell [22], cell stimulation with calcium mobilization (through VGCCs activation) [23] and apoptosis (cell death) [24], [25], [26], [27]. The main issue with these results however is that they suggest a very low efficiency of processing for a PEF having a relatively low peak value, say around 25 kV/cm, as it is expected to be generated in a deep tissue by a *contactless* reflector-based system. In such conditions, to obtain the effect on a significant percentage of cells, it was necessary to apply an extremely large number of pulses, of the order of a few millions [22].

The development of *contactless* PEF technologies has been a major research theme in the long history of an ongoing collaboration between Pau University and Loughborough University and two major works have been already published discussing a novel technique for food processing [28] and a subnanosecond driven prolate antenna operated underwater [29]. The latter work reports the first practical demonstration of generating underwater a peak PEF of 50 kV/cm at 8 cm away from any metallic structure i.e., fulfilling the conditions required for *contactless* deep tissue permeabilization [17].

The arrangement reported here is using a standard electrode-based approach. In the preliminary phase of this study, it was decided to apply PEFs on the *E. Coli* DH5α bacteria, which are very small cells with a diameter in the range of 1 μm.

Firstly, the pulsed power generator will be introduced, together with its corresponding diagnostics.

Secondly, a detailed 3-D model is presented, based on the CST Microwave Studio, a 3-D finite integral time-domain (FITD) electromagnetic simulation software [30]. As the direct measurement of the PEF generated inside a cuvette containing the cell culture is technically challenging, a comprehensive 3-D modelling and numerical electromagnetic analysis were essential during the experimental studies.

Thirdly, we report encouraging preliminary results that demonstrate that a high percentage of permeabilized bacteria can be achieved using the described arrangement.

The paper ends with conclusions and a brief presentation of the way ahead.

II. EXPERIMENTAL ARRANGEMENT

For the present studies, a pulsed power generator similar to that described in [31] was adapted for use as a subnanosecond transient source capable of producing high voltage pulses with an amplitude of up to 20 kV and having a 100 ps rise time on a 50 Ω matched load, with a duration of about 600 ps. The generator is connected to the PEF processing load through a 2.5 m long RG214-U type coaxial 50 Ω cable, having an insulator made of polyethylene with relative permittivity of 2.26. A simplified scheme of the pulsed power arrangement is shown in Fig. 1. The generator is constructed as a fast pulse forming line, with the closing switch operated under high-pressure air. To obtain a 20 kV peak voltage output, the product of the air pressure and the gap distance of the electrode system was held to 37 bar · mm. This value was then adjusted to obtain other values for the output peak voltage. The output voltage is measured using a capacitive voltage divider, the main voltage probe, attached to the RG214-U coaxial cable (Fig. 1b). The transmission coefficient for this probe is equal to -46 dB all over the frequency bandwidth and the reflection coefficient is lower than -12 dB while the cut-off frequency is close to 6 GHz.

The PEF processing load connected at the end of the RG214-U coaxial cable (Fig. 1b) consists of two parallel-plate electrodes made of copper. The distance between copper electrodes is fixed to 12 mm to allow mounting between them a standard electroporation cuvette, having a gap distance of 4 mm between its internal aluminium electrodes. The volume of the sample which contains the deionized water to be tested was kept at 100 μL for two reasons. Firstly, to obtain the desired PEF in water in terms of amplitude, rise time and duration and secondly to reduce the impedance mismatch. To avoid any possible electric

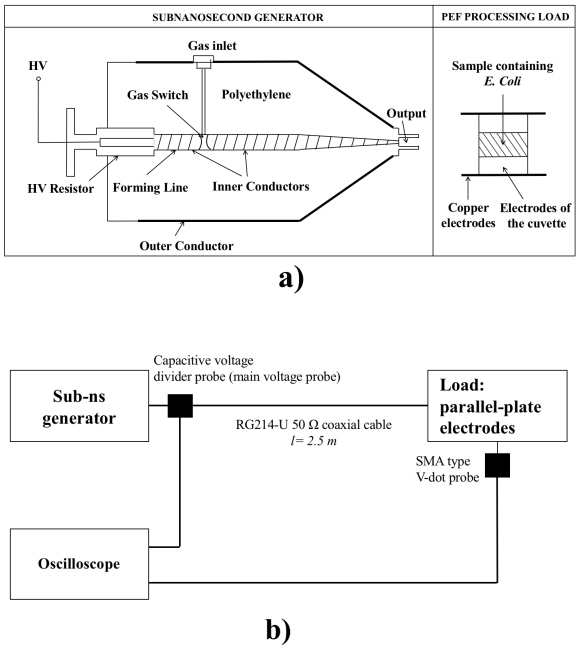

Fig. 1. Pulsed power arrangement for subnanosecond PEF. a) Subnanosecond generator (adapted after [31]) and PEF processing load and b) overall schematic.

breakdown, the upper part of the cuvette was additionally filled with 1.6 mL of paraffin oil, having a relative permittivity 2.33. It is important to note that the dielectric strength of the present experimental arrangement, when subnanosecond electric pulses are applied, is much higher compared to cases when 50 Hz AC, microsecond or longer duration pulses are applied. The complete experimental configuration is presented in Fig. 2. A SMA-type V-dot probe is mounted just a few millimetres below the cuvette with the connector's body attached to the ground plate electrode. This probe is used to control the voltage across the cuvette, with the electric field in the cuvette obtained using the numerical technique described below.

III. Numerical techniques

A detailed 3-D modeling and EM analysis were carried out for the PEF system. To shorten the time required for numerical analysis of the 50 Ω (RG214-U) coaxial cable, only a length of 101 mm was considered, corresponding to a propagation time of 0.5 ns. The 3-D CST model of the PEF processing load is presented in Fig. 3. The presence of the bacteria in the water contained inside the cuvette was not taken into consideration in the CST simulation, as measurements of electrical permittivity and the real signals recorded from the SMA-type V-dot probe, both demonstrated the bacteria do not introduce a significant difference. To analyse the impedance profile along the coaxial cable and in the PEF processing load and to better understand its behaviour due to the presence of the electroporation cuvette, we have numerically performed the Time Domain Reflectometry (TDR) task in CST. The TDR was evaluated based on the reflected signals using the integrated Gaussian signal shown in Fig. 4, with a rise time of 219 ps and a frequency bandwidth of 4 GHz, following the formula:

$$Z(t) = Z_0 \frac{\int_0^\infty i(\tau)d\tau + \int_0^t o(\tau)d\tau}{\int_0^\infty i(\tau)d\tau - \int_0^t o(\tau)d\tau} \quad (1)$$

where Z_0 is the characteristic impedance of the coaxial cable i.e., 50 Ω, $i(t)$ is the incident signal at CST Port 1 (Fig. 3) and $o(t)$ is the reflected signal at the same port. Fig. 5 shows the impedance is 50 Ω along the coaxial cable and then at 1 ns, which corresponds to the return end of the coaxial cable, the impedance starts to increase to a value of 70 Ω. This effect is due to the *mismatch* between the coaxial cable and the PEF processing load. At around 1.2 ns the impedance starts to decrease and at 1.4 ns attains a minimum value of 32 Ω. This impedance decrease is due to the cuvette, which is placed at a distance of 121 mm from the coaxial cable input (Port 1). At around 1.8 ns the impedance again increases rapidly this time due to the open end of the PEF load. Both incident and reflected signals at Port 1 were carefully analysed to observe the impedance distribution within the electric assembly. In addition, the estimation of the TDR allows us to have a representation of the time variation of the PEF processing load reflection coefficient (Fig. 6).

The electric field distribution inside the cuvette was studied using the CST Electrostatics solver. The cuvette behaves like a collection of two parallel plate capacitors mounted in parallel, one containing paraffin oil and the other water. Because of this, the electric field strength is the same in the two media, but the displacement fields are different. CST calculations indicate for the cuvette a total equivalent capacitance of 5.95 pF, a value allowing voltage pulses having about 258 ps rise time to be delivered to the PEF processing load.

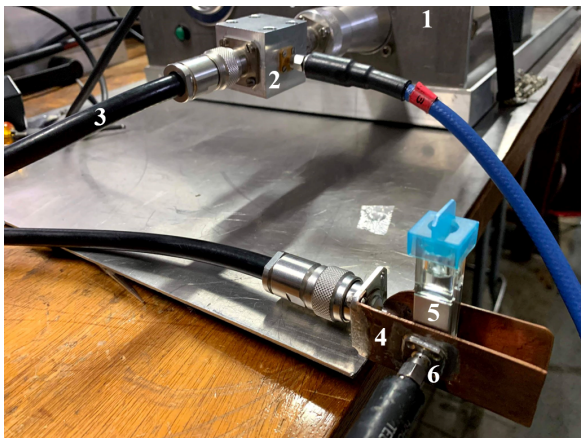

Fig. 2. Experimental arrangement for subnanosecond PEF processing. The numbers 1 to 6 represent the generator (1), capacitive voltage divider (main voltage probe) (2), RG214-U 50 Ω coaxial cable (3), two parallel-plate electrodes (4), 4 mm electroporation cuvette (5) and SMA-type V-dot probe (6).

IV. DETERMINATION OF THE TIME VARIATION OF THE ELECTRIC FIELD IN THE PROCESSED WATER SAMPLE

Because of the very small size of the water sample to be processed, there are no available techniques that can be used to directly measure the electric field generated inside. The only way to determine this essential parameter, which allows the correct interpretation of the biological results, is to use a combination of numerical modelling predictions and experimental evidence. Firstly, a detailed 3-D CST electromagnetic analysis of the load was carried out, including the SMA-type V-dot probe mounted near the cuvette (Fig. 7). The input signal applied to the processing load (see Fig. 8) was accurately measured using the main voltage probe attached to the RG214-U coaxial cable described above. This experimentally obtained voltage signal, with a rise time of about 258 ps and FWHM about 434 ps, was then used as an input (or excitation signal) for the CST Port 1 situated at the coaxial cable input (Fig. 3). To check the model, the predicted reflected signal was then successfully compared with the experimentally recorded reflected signal (see Fig. 9). To allow this comparison, the time delay of the signal due to the 2.5 m coaxial cable (see Fig. 8) was adjusted to the corresponding shorter time delay of only 101 mm length of cable considered by the CST model (see Fig. 9). A second comparison between CST predictions and the experimental data was performed for the CST Port 2 situated at the V-dot probe output (Fig. 3). Fig. 10 demonstrates the very good similarity between the predicted and the measured signal.

The above presented preliminary work had two important consequences:

i) Following [32], the SMA-type V-dot probe could be calibrated, with the voltage $V(t)$ calculated from the probe output voltage signal $V_{signal}(t)$ as:

$$V(t) = \frac{1}{\tau}\int_0^t V_{signal}(t)dt \qquad (2)$$

where $\tau = Z_0 \cdot C_1$, with Z_0= 50 Ω being the impedance of the cable connecting the probe to oscilloscope and C_1= 2.9 fF the probe coupling capacitance [32] [33], as shown in Fig. 7 was obtained using CST calculations.

ii) The following procedure was established. *During testing, the electric field generated inside the water sample is calculated by CST, using an input voltage Port 1 based on the experimentally measured input voltage signal.* However, as a precaution, the CST predictions for Port 2 are always checked against the experimental signal generated by the V-dot probe housed inside the load. If the two are identical, the CST results are most likely correct. If the two are different, a possible explanation could be that electric breakdowns are present inside the processing load.

As an example, Fig. 11 presents the calculated time variation of the electric field strength inside the water

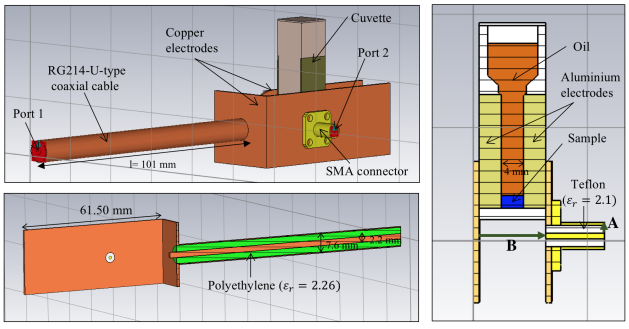

Fig. 3. Complete CST model for the PEF processing chamber, including the RG214-U coaxial cable, the two parallel-plate copper electrodes with the SMA-type V-dot probe attached and the electroporation cuvette, with various compartments filled with paraffin oil and water sample, which may contain bacteria. The two CST ports are highlighted.

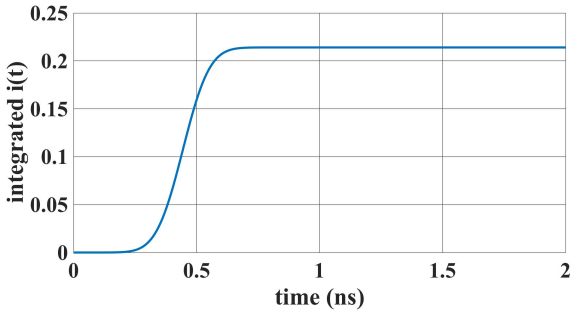

Fig. 4. Integrated Gaussian signal used to perform the TDR task.

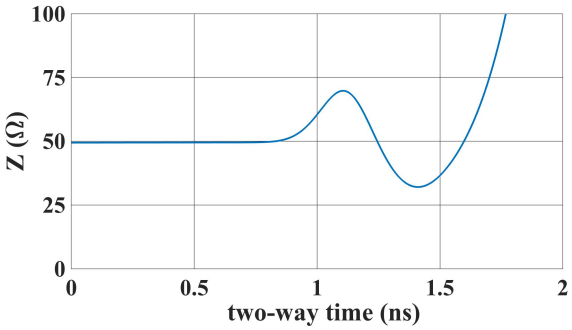

Fig. 5. The impedance profile along the cable and the processing load.

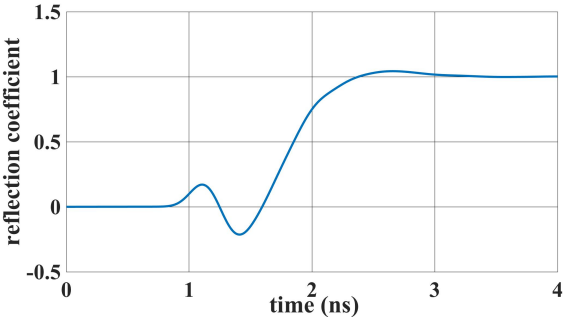

Fig. 6. Time variation of the reflection coefficient for the PEF processing load.

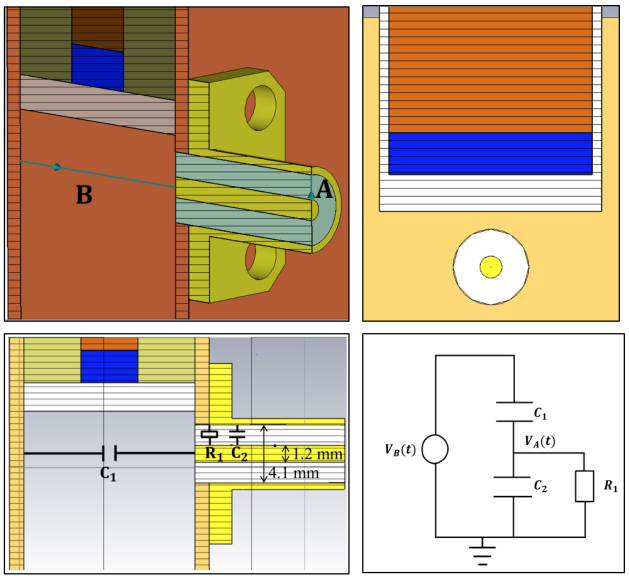

Fig. 7. *Upper*: V-dot probe mounted inside the PEF load, near the cuvette containing the water to be processed. *Lower*: its corresponding equivalent electric scheme, following that described in [32] [33].

sample for the experimental conditions of Fig. 9 i.e., when the peak transient voltage input reaches a peak of 20 kV. The corresponding peak electric field strength reaches 61 kV/cm, with a rise time of 338 ps and a FWHM of 823 ps. At this moment, the corresponding electric field distribution inside the processing load is shown in Fig. 12. It is important to note two essential characteristics:
- the electric field is mainly concentrated inside the cuvette.
- inside the cuvette the electric field is highly homogeneous, allowing a simple interpretation of the results obtained after PEF processing.

When performing a large number of tests at a high PRF, one important question is related to the possible temperature increase of the water sample. The variation of temperature ΔT during N consecutive shots is given by:

$$\Delta T = \frac{W}{mC_p} N \tag{3}$$

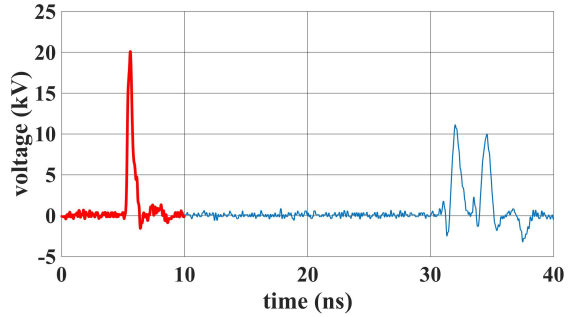

Fig. 8. The complete signal recorded from the main voltage probe considering the total length of 2.5 m for the RG214-U coaxial cable. The first 10 ns of the experimental voltage signal (highlighted) are used as CST input data.

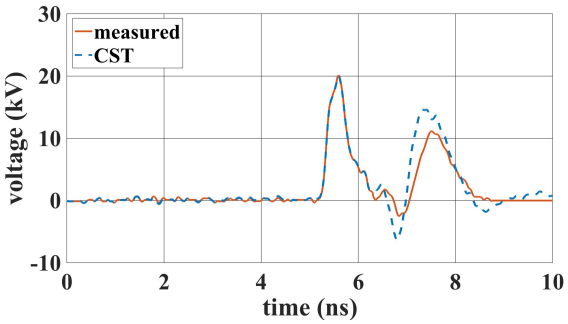

Fig. 9. *Full line*: experimental signal obtained from the main voltage probe. *Dotted line*: CST prediction for the voltage at Port 1.

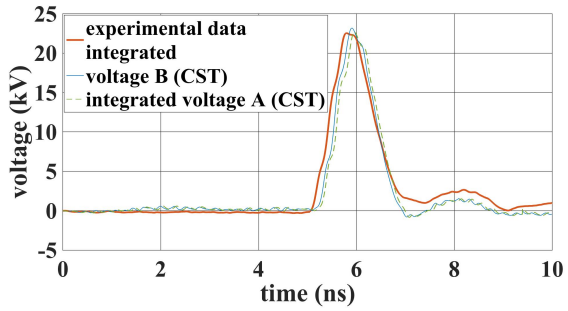

Fig. 10. Second comparison between CST model and experimental data. *Thick line*: time dependence of the integrated voltage signal from V-dot probe. *Thin line*: CST prediction obtained from a virtual voltage probe placed at location B. *Dotted line*: integrated voltage signal output from Port 2 placed at location A. The location of both A and B is presented in Fig. 7. The two CST generated traces are practically indistinguishable demonstrating that, due to the favourable electric field distribution, the SMA probe acts indeed as a V-dot probe [33].

where W is energy deposited in the water during one shot, $m \approx 100$ mg is the mass of the water sample and $C_p = 4188$ J/kg/K is the constant-pressure heat capacity of water at 25 °C [34]. The energy is calculated as:

$$W = R\int_0^t I^2(t')dt' \tag{4}$$

where R is the water sample resistance while the current in-

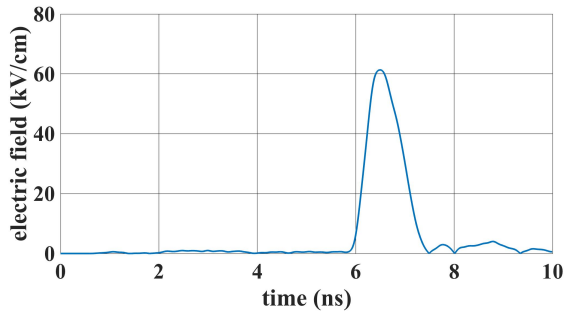

Fig. 11. The PEF parameters generated inside the cuvette water sample, for the input conditions of Fig. 9. The peak electric field strength is reaching 61 kV/cm, with a rise time of 338 ps and a FWHM of 823 ps.

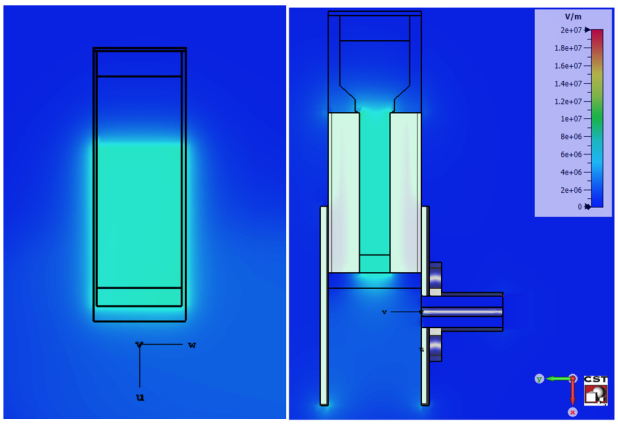

Fig. 12. The electric field distribution inside the processing load at the moment the peak field of 61 kV/cm is generated inside the cuvette water sample (see Fig. 11).

tegral was performed using data from a CST virtual current sensor. As the water sample has a conductivity of about σ = 300 µS/m and a relative permittivity ε_r = 78.4 at 25 °C [35], the time constant $\varepsilon_0\varepsilon_r/\sigma$ = 140 µs is much larger than the pulse duration (≈ 2 ns) and therefore the conduction current can safely be ignored. In such conditions the water series equivalent resistance can be estimated as:

$$R = \frac{tan\delta}{2\pi f C_w} = 1.28\,\Omega \tag{5}$$

where tanδ = 0.005 [35] is the water loss tangent at a frequency f estimated as $f = 0.35/t_{rise}$ = 1.35 GHz, where t_{rise} = 258 ps is the rise time of the impulse. The equivalent capacitance C_w of the water sample was calculated using CST as C_w = 4.6 pF. As a typical result, after applying N = 50000 consecutive shots, the estimated water sample temperature increase is only ΔT = 0.00615 °C and therefore negligible.

V. Biological techniques

E. Coli DH5α were purchased from Invitrogen (Courtaboeuf, France). Cultures used for experiments were grown from 80 µL of bacterial stock solution (saturated bacterial broth mixed with glycerol in (1:1) ratio stored at -80 °C) added to 8 mL of Luria Bertani (LB) medium (Invitrogen LB broth base Lennox L) and incubated at 37 °C under constant orbital shaking at 220 rpm for 8 hours over day, corresponding to an endpoint OD600 of approximately 0.9. Cultures were then placed at 4 °C overnight until used for experiments on the next day. *E. Coli* permeabilization was assessed using a cell-impermeant fluorescent nucleic acid stain entering only permeabilized bacteria, the YO-PRO^{TM}-1 iodide (λ_{ex} 491/ λ_{em} 509) (Invitrogen). *E. Coli* gating in flow cytometry was validated using a cell-permeant fluorescent nucleic acid stain entering all bacteria, permeabilized or not, the SYTO® 9 (λ_{ex} 485/ λ_{em} 498) (Invitrogen). Prior to PEF exposure, bacteria were centrifuged at 2000 x g for 20 minutes, the supernatant was discarded and the bacterial pellet was resuspended in the same volume of sterile deionized water (same bacterial concentration than mother culture). Then, either YO-PRO™-1 iodide or SYTO® 9 was added (working concentrations of 30 µM and 50 µM, respectively). A volume of 100 µL of bacterial suspension with marker (YO-PRO^{TM}-1 iodide or SYTO® 9) was then placed in a 4 mm wide gap commercial electroporation cuvette (Cell Projects Ltd, Kent, UK) and covered with 1.6 mL of insulating paraffin oil in order to prevent arcing between electrodes during PEF exposure. Then, pulses were delivered at room temperature by installing the electroporation cuvette in the applicator presented in Fig. 3. Controls were sham exposures for which all the steps of the exposure protocol were followed, except for the PEF delivery. 5 minutes after PEF exposure, a volume of 50 µL of the bacterial suspension was collected from the cuvette and mixed with 50 µL of sterile deionized water. On average 30 minutes after PEF exposure, and prior to flow cytometry analyses, this bacterial suspension was mixed with 600 µL of LB medium. Flow cytometry analyses were performed using a BD Accuri™ C6 Flow Cytometer (Bd Biosciences, le Pont-de-Claix, France). An excitation laser of 488 nm and the FL1 band pass filter 533/30 were used to detect fluorescence of either YO-PRO™-1 iodide and SYTO® 9 (the reason why these markers could not be used simultaneously). For data processing, *E. Coli* were gated and separated from debris based on FSC-A and SSC-A morphological criteria. Nevertheless, a small proportion of events was not SYTO® 9 positive within this gating, meaning that there was still debris. Thus, the specificity of the gating was calculated as follow:

$$Gating\ Specificity\ (GS) = \frac{number\ of\ SYTO®9\ positive\ events}{total\ number\ of\ events} \tag{6}$$

$$\%\ permeabilized\ bacteria = \frac{\frac{\%\ of\ YO\text{–}PRO^{TM}\text{–}1\ positive\ events\ in\ sample}{GS\ sample} - \frac{\%\ of\ YO\text{–}PRO^{TM}\text{–}1\ positive\ events\ in\ control}{GS\ control}}{100 - \frac{\%\ of\ YO\text{–}PRO^{TM}\text{–}1\ positive\ events\ in\ control}{GS\ control}}\ x\,100 \tag{7}$$

TABLE I
RESULTS FROM PERMEABILIZATION EFFECT FOR VARIOUS NUMBER OF PULSES APPLIED WHEN AN ELECTRIC FIELD OF 61 KV/CM WAS APPLIED AT 200 HZ PRF.

Number of pulses applied	Mean of percentage of permeabilized bacteria (%)	Number of replicates	Standard deviation
5000	44.4	3	9.3
10000	69.4	6	12.3
25000	81	6	7.4
50000	89.3	6	4.7

The specificity of the gating was evaluated for the different experimental conditions (Sham or PEF exposures), and was considered for further data processing. Finally, the percentage of permeabilized bacteria was calculated using YO-PRO™-1 iodide following Equation 7. During our experimental study, the above chosen biological methodology was carefully followed, as it has a significant impact on the interpretation of the results. For instance, a recent study in the plasma medicine show that the treatment dose plays an important role in the biological effects observed [36].

VI. PRELIMINARY RESULTS

We assessed the ability of the subnanosecond pulses delivered by our system to induce electroporation on *E. Coli* DH5α, applying trains of 5000 to 50000 pulses at a PRF of 200 Hz at an electric field amplitude of 61 kV/cm (the top electric field amplitude deliverable with the present arrangement). Several replicates were performed (replicates are the number of experimental units in a treatment) and the corresponding standard deviation was calculated (see Table I). All conditions tested efficiently generated electroporation of the bacteria to YO-PRO™-1 iodide, a fluorescent nucleic acid stain and cell permeabilization marker of approximately 630 Da. Moreover, under these conditions, we observed an additive effect of the pulses, the percentage of permeabilized bacteria increasing from 44.4 % ± 9.3 % to 89.3 % ± 4.7 % for 5000 to 50000 pulses applied, respectively (Table I). Importantly, no increase of the temperature within the samples submitted to PEF treatment was noticed under the conditions tested in this study, in line with the estimated temperature rise presented above under Section IV. Thus, the permeabilization of *E. Coli* observed in response to PEF exposure performed in this study cannot be attributed to thermal effects.

VII. CONCLUSION AND THE WAY AHEAD

A relatively simple arrangement for PEF processing driven by a subnanosecond pulsed power generator has been developed and tested. The preliminary results show that subnanosecond processing can be highly efficient. The way ahead will require the development of a compact, high PRF and mobile subnanosecond 0.5 MV pulsed power generator that, when coupled with a prolate reflector, will allow biomedical experimentation at (or near) a hospital.

ACKNOWLEDGMENT

The authors would like to thank Valérie Bertrand and Edson Martinod from the Electrical Engineering Department of Xlim Research Institute, University of Limoges, France, for their help and discussion on CST simulations. We would also like to thank Anthony Ranchou-Peyruse from the Enviromental Microbiology Laboratory, IPREM, Université de Pau et des Pays de l'Adour (UPPA), France, for providing access to laboratory facilities.

REFERENCES

[1] K. H. Schoenbach, R. P. Joshi, J. F. Kolb, N. Chen, M. Stacey, E. S. Buescher, S. J. Beebe, and P. Blackmon, "Ultrashort electrical pulses open a new gateway into biological cells," in *Conference Record of the Twenty-Sixth International Power Modulator Symposium, 2004 and 2004 High-Voltage Workshop.*, 2004, pp. 205–209.

[2] D. Miklavčič, L. M. Mir, and P. Thomas Vernier, "Electroporation-based technologies and treatments," *The Journal of Membrane Biology*, vol. 236, no. 1, pp. 1–2, Jul 2010. [Online]. Available: https://doi.org/10.1007/s00232-010-9287-9

[3] E. Neumann, M. Schaefer-Ridder, Y. Wang, and P. H. Hofschneider, "Gene transfer into mouse lyoma cells by electroporation in high electric fields," *The EMBO journal*, vol. 1, no. 7, pp. 841–845, 1982, 6329708[pmid]. [Online]. Available: https://pubmed.ncbi.nlm.nih.gov/6329708

[4] M. J. Jaroszeski, R. Gilbert, and R. Heller, "Electrochemotherapy: an emerging drug delivery method for the treatment of cancer," *Advanced Drug Delivery Reviews*, vol. 26, no. 2, pp. 185 – 197, 1997, delivery of Chemotherapeutic Drugs. [Online]. Available: http://www.sciencedirect.com/science/article/pii/S0169409X97000343

[5] T. Murakami and Y. Sunada, "Plasmid dna gene therapy by electroporation: Principles and recent advances," *Current Gene Therapy*, vol. 11, no. 6, pp. 447–456, 2011. [Online]. Available: https://www.ingentaconnect.com/content/ben/cgt/2011/00000011/00000006/art00004

[6] D. Knorr, A. Angersbach, M. N. Eshtiaghi, V. Heinz, and D.-U. Lee, "Processing concepts based on high intensity electric field pulses," *Trends in Food Science Technology*, vol. 12, no. 3, pp. 129 – 135, 2001. [Online]. Available: http://www.sciencedirect.com/science/article/pii/S0924224401000693

[7] B. Rubinsky, "Irreversible electroporation in medicine," *Technology in Cancer Research & Treatment*, vol. 6, no. 4, pp. 255–259, 2007, pMID: 17668932. [Online]. Available: https://doi.org/10.1177/153303460700600401

[8] L. G. P. H. Vroomen, E. N. Petre, F. H. Cornelis, S. B. Solomon, and G. Srimathveeravalli, "Irreversible electroporation and thermal ablation of tumors in the liver, lung, kidney and bone: What are the differences?" *Diagn Interv Imaging*, vol. 98, no. 9, pp. 609–617, Sep 2017.

[9] R. V. Davalos, B. Rubinsky, and L. M. Mir, "Theoretical analysis of the thermal effects during in vivo tissue electroporation," *Bioelectrochemistry*, vol. 61, no. 1, pp. 99 – 107, 2003. [Online]. Available: http://www.sciencedirect.com/science/article/pii/S156753940300080X

[10] K. Nurgali, R. T. Jagoe, and R. Abalo, "Editorial: Adverse Effects of Cancer Chemotherapy: Anything New to Improve Tolerance and Reduce Sequelae?" *Front Pharmacol*, vol. 9, p. 245, 2018.

[11] J. C. Coffey, M. J. Smith, J. H. Wang, D. Bouchier-Hayes, T. G. Cotter, and H. P. Redmond, "Cancer surgery: risks and opportunities," *Bioessays*, vol. 28, no. 4, pp. 433–437, Apr 2006.

[12] C. Baum, "Focal waveform of a prolate-spheroidal impulse-radiating antenna (ira)," *Radio Science*, vol. 42, 12 2007.

[13] S. Altunc, C. E. Baum, C. G. Christodoulou, E. Schamiloglu, and C. J. Buchenauer, "Focal waveforms for various source waveforms driving a prolate-spheroidal impulse radiating antenna (ira)," *Radio Science*, vol. 43, no. 4, 2008. [Online]. Available: https://agupubs.onlinelibrary.wiley.com/doi/abs/10.1029/2007RS003775

[14] S. Altunc, C. E. Baum, C. J. Buchenauer, C. G. Christodoulou, and E. Schamiloglu, "Design of a special dielectric lens for concentrating a subnanosecond electromagnetic pulse on a biological target," *IEEE Transactions on Dielectrics and Electrical Insulation*, vol. 16, no. 5, pp. 1364–1375, 2009.

[15] S. Xiao, M. A. Migliaccio, J. C. Camp, J. F. Kolb, K. H. Schoenbach, and C. E. Baum, "A wide-band focusing system for bioelectric applications," in *2007 16th IEEE International Pulsed Power Conference*, vol. 1, 2007, pp. 744–747.

[16] R. A. Petrella, K. H. Schoenbach, and S. Xiao, "A dielectric rod antenna for picosecond pulse stimulation of neurological tissue," *IEEE Transactions on Plasma Science*, vol. 44, no. 4, pp. 708–714, April 2016.

[17] F. Guo, C. Yao, C. Bajracharya, S. Polisetty, K. H. Schoenbach, and S. Xiao, "Simulation study of delivery of subnanosecond pulses to biological tissues with an impulse radiating antenna," *Bioelectromagnetics*, vol. 35, no. 2, p. 145—159, February 2014. [Online]. Available: https://doi.org/10.1002/bem.21825

[18] S. Xiao, S. Altunc, P. Kumar, C. E. Baum, and K. H. Schoenbach, "A reflector antenna for focusing subnanosecond pulses in the near field," *IEEE Antennas and Wireless Propagation Letters*, vol. 9, pp. 12–15, 2010.

[19] P. Kumar, C. E. Baum, S. Altunc, J. Buchenauer, S. Xiao, C. G. Christodoulou, E. Schamiloglu, and K. H. Schoenbach, "A hyperband antenna to launch and focus fast high-voltage pulses onto biological targets," *IEEE Transactions on Microwave Theory and Techniques*, vol. 59, no. 4, pp. 1090–1101, 2011.

[20] M. Croizer, "Applicators destined for the studies biological effects of electrical waves subnanoseconds," Theses, Université de Limoges, Dec. 2015. [Online]. Available: https://tel.archives-ouvertes.fr/tel-01298291

[21] K. H. Schoenbach, S. Xiao, R. P. Joshi, J. Thomas Camp, T. Heeren, J. F. Kolb, and S. J. Beebe, "The effect of intense subnanosecond electrical pulses on biological cells," *IEEE Transactions on Plasma Science*, vol. 36, no. 2, pp. 414–422, 2008.

[22] S. Xiao, S. Guo, V. V. Nesin, R. Heller, and K. H. Schoenbach, "Cell membrane permeabilization and death caused by subnanosecond electric pulses," in *2010 IEEE International Power Modulator and High Voltage Conference*, 2010, pp. 194–199.

[23] I. Semenov, S. Xiao, D. Kang, K. H. Schoenbach, and A. G. Pakhomov, "Cell stimulation and calcium mobilization by picosecond electric pulses," *Bioelectrochemistry*, vol. 105, pp. 65–71, Oct 2015.

[24] S. Xiao, S. Guo, V. Nesin, R. Heller, and K. H. Schoenbach, "Subnanosecond electric pulses cause membrane permeabilization and cell death," *IEEE Trans Biomed Eng*, vol. 58, no. 5, pp. 1239–1245, May 2011.

[25] J. T. Camp, Y. Jing, J. Zhuang, J. F. Kolb, S. J. Beebe, J. Song, R. P. Joshi, S. Xiao, and K. H. Schoenbach, "Cell death induced by subnanosecond pulsed electric fields at elevated temperatures," *IEEE Transactions on Plasma Science*, vol. 40, no. 10, pp. 2334–2347, 2012.

[26] Y.-Y. Hua, X.-S. Wang, Y. Zhang, C.-G. Yao, X.-M. Zhang, and Z.-A. Xiong, "Intense picosecond pulsed electric fields induce apoptosis through a mitochondrial-mediated pathway in hela cells," *Molecular medicine reports*, vol. 5, no. 4, pp. 981–987, Apr 2012, 22307872[pmid]. [Online]. Available: https://pubmed.ncbi.nlm.nih.gov/22307872

[27] J. Jia, Z.-A. Xiong, Q. Qin, C.-G. Yao, and X.-Z. Zhao, "Picosecond pulsed electric fields induce apoptosis in a cervical cancer xenograft," *Molecular medicine reports*, vol. 11, no. 3, pp. 1623–1628, Mar 2015, 25405328[pmid]. [Online]. Available: https://pubmed.ncbi.nlm.nih.gov/25405328

[28] B. M. Novac, F. A. Banakhr, I. R. Smith, L. Pécastaing, R. Ruscassié, A. S. de Ferron, and P. Pignolet, "Demonstration of a novel pulsed electric field technique generating neither conduction currents nor joule effects," *IEEE Transactions on Plasma Science*, vol. 42, no. 1, pp. 216–228, 2014.

[29] B. M. Novac, R. Xiao, P. Senior, L. Pécastaing, and I. R. Smith, "Generation of intense pefs using a prolate spheroidal reflector attached to the bipolar former of a 10-gw pulsed power generator," *IEEE Transactions on Plasma Science*, vol. 46, no. 10, pp. 3547–3551, Oct 2018.

[30] "Computer simulation technology," https://www.3ds.com/, accessed: 2020-04-28.

[31] L. Pécastaing, J. Paillol, T. Reess, A. Gibert, and P. Domens, "Design and performance of high voltage pulse generators for ultra-wideband applications," *Measurement Science and Technology*, vol. 12, no. 10, pp. 1718–1725, sep 2001. [Online]. Available: https://doi.org/10.1088%2F0957-0233%2F12%2F10%2F316

[32] C. A. Ekdahl, "Voltage and current sensors for a high-density z-pinch experiment," *Review of Scientific Instruments*, vol. 51, no. 12, pp. 1645–1648, 1980. [Online]. Available: https://doi.org/10.1063/1.1136140

[33] B. M. Novac, R. Xiao, T. Huiskamp, L. Pécastaing, M. Wang, P. Senior, A. S. de Ferron, A. J. M. Pemen, and M. Rivaletto, "Theoretical and experimental studies of off-the-shelf v-dot probes," *IEEE Transactions on Plasma Science*, vol. 46, no. 8, pp. 2985–2992, 2018.

[34] M. W. Chase, *NIST-JANAF Thermochemical Tables, Fourth Edition*. Journal of Physical and Chemical Reference Data, Monograph 9, pp. 1-1951 , 1998.

[35] M. Zahn, Y. Ohki, D. B. Fenneman, R. J. Gripshover, and V. H. Gehman, "Dielectric properties of water and water/ethylene glycol mixtures for use in pulsed power system design," *Proceedings of the IEEE*, vol. 74, no. 9, pp. 1182–1221, 1986.

[36] H. Cheng, J. Xu, X. Li, D. Liu, and X. Lu, "On the dose of plasma medicine: Equivalent total oxidation potential (etop)," *Physics of Plasmas*, vol. 27, no. 6, p. 063514, 2020. [Online]. Available: https://doi.org/10.1063/5.0008881

Njomza Ibrahimi (S'19) received the B.Sc degree in Electrical Engineering from the University of Pristina, Kosovo, in 2015. The M.Sc degree was obtained from the same University in 2017, combined with a one-year exchange study/research period at the Norwegian University of Science and Technology, Gjøvik, Norway. Currently, she is working towards the Ph.D degree in the Department of Electrical Engineering of Université de Pau et des Pays de l'Adour (UPPA), Pau, France. Her research interests include high-voltage pulsed power systems and high-power microwave generation and transmission and their application in the biomedical domain.

Leslie Vallet received the M.Sc degree in Chemical Engineering from CPE Lyon Engineering School, France, in 2018, associated with one-year exchange study period at Ecole Polytechnique Fédérale de Lausanne, Switzerland, specializing in Biology. She is currently doing her Ph.D in METSY Unit at Gustave Roussy European Cancer Centre, France. Her research interests includes the interactions between biological cells and electric fields for medical application purposes.

Franck Andre received the master degree in Engineering (Science for Biological and Food Industries) from the Paris Institute of Technologies AgroParisTech (ex INA P-G), Paris, France, in 2002. He obtained the PhD degree for his research performed on in vivo gene electrotransfer from the Paris Institute of Technologies AgroParisTech (ABIES Doctoral School) in 2006. During his postdoc (2007-2009) at the Frank Reidy Research Center for Bioelectrics (Old Dominion University, Norfolk, Virginia, USA) he investigated the effects of nanosecond pulsed electric fields on cell and nuclear membrane permeabilization. He is currently a Researcher in the French National Centre for Scientific Research (CNRS). For the last few years his research has been mainly focused on electroporation - based gene transfer and drug delivery, and on the use of electric pulses to manipulate the cytosolic calcium oscillations.

Laurent Ariztia received both B.Sc and M.Sc degree from the Université de Pau et des Pays de l'Adour (UPPA), Pau, France, in 2017 and 2019, respectively. He is currently an Engineer at SIAME Laboratory. His research interests are mainly focused on pulsed power systems such as Marx generators and pulse forming lines for military and civil applications.

Marc Rivaletto was born in Tarbes, France, in 1960. He graduated from Supelec Electrical Engineer School in 1984 and received the Ph.D. degree in electrical engineering from Pau University, Pau, France, in 1997. He is currently a Lecturer at Pau University and works in the SIAME Laboratory. His research interests are HPM sources, compact pulsed power systems, including pulse forming lines, compact Marx generator and resonant transformer.

Antoine Silvestre de Ferron was born in Tarbes, France, in 1977. He received the master degree in electrical and electronic engineering from the University of Toulouse, Toulouse, France, and the Ph.D. degree in electrical engineering from the University of Pau, Pau, France, in 2002 and 2006, respectively. From 2006 to 2008, he was a Researcher with the Atomic Energy Commission (CEA), a French government-fund technological research organization in Le Barp, France. He is currently an engineer in the electrical engineering laboratory of the University of Pau, France. His research interests include pulsed power generation, with military and civil applications and the high voltage transient probes associated.

Bucur M. Novac (M'06 - SM'08) received the M.Sc. and Ph.D. degrees in 1977 and 1989, respectively, both from the University of Bucharest. He joined the Loughborough University, UK in 1998 and is currently Professor of Pulsed Power. His research interests include compact and repetitive high-power systems, explosively and electromagnetically driven magnetic flux compression generators and their applications, electromagnetic launchers, ultrafast magneto and electro-optic sensors and 2-D modeling of pulsed-power systems. He has co-authored two books on explosive pulsed power and has published more than 200 refereed papers and conference contributions. Prof. Novac is a voting member of the Pulsed Power Science Technology Committee in the IEEE Nuclear and Plasma Science Society. He is also a member of the International Steering Committees for both the MEGAGAUSS Conferences and for the Euro-Asian Pulsed Power Conferences. He is also co-chairman of the UK Pulsed Power Symposium. Prof. Novac is a Fellow of the Royal Academy of Engineering, a Chartered Engineer and a Fellow of The Institution of Engineering and Technology (IET), all UK.

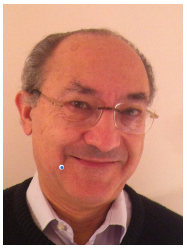

Dr. Lluis M. Mir did his graduate work at Ecole Normale Supérieure (Paris) and obtained his D.Sc. at Univ. of Toulouse in 1983. In 2018 he received three Doctorate Honoris Causa, from the Universities of Buenos Aires (Argentina), Lima (Peru) and Ljubljana (Slovenia). DRCE at CNRS, he directed the Laboratory of Vectorology and Anticancer Therapies (2010-2019) and the European Associated Laboratory for the applications of Electric pulses in Biology And Medicine (2011-2018). Fellow of the American Institute for Medical and Biological Engineering, the European Academy of Tumor Immunology and the RadioScience International Union (URSI), he published 238 peer-reviewed articles and 25 book chapters (H index=70, WoS). He won several awards, including the URSI's 2017 Balthasar van der Pol Gold Medal. He is the present President of the International Society for the Electroporation Based Treatments and Therapies.

Laurent Pécastaing (M'13-SM'17) received the Ph.D. degree and the Research Directorship Habilitation in electrical engineering from the Université de Pau et des Pays de l'Adour (UPPA), Pau, France, in 2001 and 2010, respectively. He is currently a Full Professor in pulsed power with the Laboratoire SIAME, UPPA. He is the Head of the High Voltage Processes team with the Laboratoire SIAME and he is also the Director of a Common Laboratory with the CEA, France. His current research interests include high-power microwave sources, compact pulsed power systems and ultrafast transient probes. Prof. Pécastaing is the Chairman of the next EAPPC/BEAMS/MEGAGAUSS Conference to be held in France in 2021. He is also a member of the International Steering Committees for both the BEAMS Conferences and for the Euro-Asian Pulsed Power Conferences.